

## Human Umbilical Cord Mesenchymal Stem Cells Ameliorate Silver Nanoparticles Induced Sub-chronic Lung toxicity in Adult Male Albino Rats

Arwa A. El-Sheikh<sup>1</sup>, Samaa Salah Abd El-Fatah<sup>2</sup>, Rania Said Moawad<sup>2</sup> and Doaa Mohammed Yousef<sup>2</sup>

<sup>1</sup>Forensic Medicine and Clinical Toxicology Department, Faculty of Medicine, Zagazig University, Egypt.

<sup>2</sup>Anatomy and Embryology Department, Faculty of Medicine, Zagazig University, Egypt.

[Samaasalih12@yahoo.com](mailto:Samaasalih12@yahoo.com)

**Abstract: Background:** Silver nanoparticles (Ag-NPs) are nanomaterials that become used widely in several applications and products. **Objective:** The current work aimed at studying the Ag-NPs effects on the lung tissues of adult male albino rats and to evaluate the potential ameliorating role of human umbilical cord mesenchymal stem cells (HUCMSCs) through biochemical, histopathological, immunohistochemical and ultra-structural lung tissues examinations. **Material and methods:** thirty adult male albino rats were divided into control groups (I), Ag-NPs group (II), received (300mg/kg) of Ag-NPs orally by gavage and Ag-NPs+ HUCMSCs (III), received Ag-NPs as group II and (0.5 × 10<sup>6</sup>)/80 µl PBS of HUCMSCs by intravenous injection in rat tail vein for the two successive days after 4 weeks of AG-NPs administration. Lung tissues samples were examined for Nitric oxide (NO), Myeloperoxidase (MPO) activities and reduced glutathione (GSH) content. Moreover the histopathological, ultra-structural and immunohistochemical examinations were performed. **Results:** Ag-NPs induced oxidative stress by increased NO, MPO activities, inducible nitric oxide synthase (iNOS) expressing cells and decreased GSH contents in lung tissues. In additionally, Ag-NPs caused histopathological and ultra-structural alterations. HUCMSCs restored most of histological and ultra-structural architecture. Furthermore, reduced NO, MPO activities, iNOS expressing cells and increased GSH contents of lung tissues. **Conclusion:** HUCMSCs have a potential promising role in improving oxidative stress caused lung injury induced by Ag-NPs in adult male rats.

[Arwa A. El-Sheikh, Samaa Salah Abd El-Fatah, Rania Said Moawad and Doaa Mohammed Yousef. **Human Umbilical Cord Mesenchymal Stem Cells Ameliorate Silver Nanoparticles Induced Sub-chronic Lung toxicity in Adult Male Albino Rats.** *Life Sci J* 2018;15(10):43-54]. ISSN: 1097-8135 (Print) / ISSN: 2372-613X (Online). <http://www.lifesciencesite.com>. 5. doi:[10.7537/marslsj151018.05](https://doi.org/10.7537/marslsj151018.05).

**Keywords:** Silver nanoparticles, human mesenchymal stem cells, nitric oxide, Myeloperoxidase, ultra-structural, lung

### 1. Introduction

Nanotechnology was included in different areas as biotechnology, molecular and cellular biology, reproduction, drug delivery and pathogen detection. Silver Nanoparticles (Ag-NPs) are from the commonest used various nanoparticles due to its antibacterial, antiviral and antifungal activities (Reidy et al., 2013).

Silver Nanoparticles used in multiple applications as food, clothing, cosmetics, electronics and medical devices (Wijnhoven et al., 2009). It was observed that nanomaterials produced cytotoxicity despite of their effectiveness in industry, based on different factors as particle size, surface chemistry and morphology (Iavicoli et al., 2013). Nanomaterials induced toxicity either by disrupting mitochondrial function producing oxidative stress or by apoptosis resulting in membrane damage (BraydichStolle et al., 2005).

The small size and surface area of Ag-NPs allow them to pass through cell membranes and biological barriers causing cellular dysfunction (Xia et al., 2008). Synthesis of Ag-NPs generally involves the use of surface coatings agents to protect silver ions from

oxidation and dissolution of agglomeration of particles, Polyvinylpyrrolidone (PVP) is commonly-used coating agent imparting negative charge (Seiffert et al., 2015). Several studies reported pulmonary toxic effects of Ag-NPs by tracheal instillation (Seiffert et al., 2015; Wiemann et al., 2017).

Stem cells are undifferentiated cells, with capability for clonality, self-renewal, and the potential to differentiate into different types of cells and tissue (Kolios and Moodley, 2013). Mesenchymal stem cells (MSCs) therapy has been demonstrated recently in many diseases, reporting its effectiveness. Previous studies focused on the paracrine properties of MSCs in limiting acute lung injury and enhancing lung repair (Krause et al., 2001; Lee et al., 2009).

In the current study, we wanted to evaluate the role of HUCMSCs in Ag-NPs induced sub chronic lung toxicity in adult rats by investigating oxidative stress products, light and electron histopathological and immunohistochemical alterations in lung tissues of adult rats.

### 2. Material and Methods

#### Chemicals

Silver nanoparticles (Ag-NPs) were purchased from (Sigma -aldrichchemical Company, St. Louis, MO, USA) as brown odorless fine nano- powder dissolved in polyvinyl pyrrolidone (PVP) as dispersant with particle size <100 nm and purity  $\geq 99.5\%$  trace metals basis. The CAS No is 7440-22-4. Distilled water was used as a solvent.

The chemicals and reagents used were of analytical grade as Nitric Oxide Assay Kit (Colorimetric, ab65328) used for measurement of Nitric oxide (NO) levels was purchased from (Abcam Company, Cairo, Egypt). Myeloperoxidase (MPO) activity assay by (Fluorometric Assay Kit) obtained from (SigmaChemical Company, St. Louis, MO, USA). Reduced glutathione (GSH) was assayed by Biocon Diagnostik kit (GmbH, Vohl-Marienhagen, Germany).

### Animals

Thirty adult male albino rats were obtained from Animal House of Faculty of Medicine, Zagazig University with an average body weight of 160-200gm and average age 8-10 weeks. The rats were housed in plastic cages with stainless steel wire-bar lid under standard conditions (temperature  $23\pm 2^\circ\text{C}$ , humidity  $50\pm 5\%$ , 12:12h light/dark cycle). The rats were left to adapt for 1 week before the experiment. All the ethical issues were considered based on the medical research ethics committee of faculty of medicine, Zagazig University, Egypt.

### Human umbilical cord Mesenchymal Stem Cells (HUCMSCs)

Human umbilical cord blood was collected from full-term delivery women at Gynaecology Department, Zagazig University Hospitals, Zagazig, Egypt.

### Experimental Design

Animals were divided into Group I (Control groups): 18 rats equally divided into three subgroups, A: received no treatment, B: received once daily dose of 0.5 ml Distilled water (vehicle of Ag-NPs) by oral gavage. C: received 0.5 ml of phosphate buffer saline (PBS) (vehicle of MSCs) by intravenous injection into the tail vein.

Group II (Ag-NPs received group): 6 rats received a daily dose (300mg/kg) of Ag-NPs (Kim et al., 2012) dissolved in 0.5 ml of distilled water 6 day/week by oral gavage for 4 weeks.

Group III (Ag-NPs +HUCMSCs): 6 rats received the same dose of Ag-NPs by the same route and for the same duration. After (4 weeks of AG-NPs administration), the rats received a dose of  $0.5 \times 10^6$  of HUCMSCs suspended in 80  $\mu$ l phosphate buffer saline (PBS) by intravenous injection in rat tail vein for the two successive days (Zhu et al., 2017).

At the end of the experiment, the animals of all studied groups had been fasted over-night; each animal was anesthetized with ether. The animals were

then euthanized by cervical dislocation and lungs were excised and multiple lung sections were dissected. Portion of each section subjected to histopathological and immunohistochemical staining, ultra-structural examination and oxidative products assessment.

### Human umbilical cord Mesenchymal Stem Cells isolation

MSCs extraction was performed according to (Secunda et al., 2015) in Stem Cell Lab, Medical Biochemistry and Molecular Biology Department, Faculty of Medicine, Zagazig University, Egypt. Human umbilical cord blood was collected under strict aseptic conditions into blood collection bag containing citrate phosphate dextrose anticoagulant from full-term delivery women at Gynaecology Department, Zagazig University Hospital, Zagazig, Egypt, within formed consent.

Human umbilical cord blood was diluted with 1:3 of PBS buffer. Isolation of mononuclear cells (MNCs) was by addition of 20 ml of diluted blood into 10 mL of Ficoll/Paque Lymphocyte Separation Medium (Lonza Bioproducts, Basel, Switzerland) in centrifuge tubes then, centrifuged at room temperature for 20 min. The interphase MNCs layer collected after aspirating and discarding the supernatant. The cells were rewashed twice with PBS and centrifuged at room temperature. The cells were re-suspended in the isolation media and transferred to culture dishes. The isolation media was high glucose Dulbecco's Modified Eagle's Medium with glucose (4.5 g/L), L-glutamine (Lonza Bioproducts, Basel, Switzerland) and 10% fetal bovine serum (FBS, Lonza Bioproducts, Basel, Switzerland) supplemented with 1% penicillin, streptomycin, Amphotericin B Mixture (10 IU/10 IU/25 mg, 100 mL) Lonza Bioproducts, Basel, Switzerland). Cells were incubated at  $37^\circ\text{C}$  in 5% humidified CO<sub>2</sub> incubator (Heraeus, Langensfeld, Germany). Non-adherent cells were eliminated by a medium change every 2 days. The cells were grown for 2 weeks as a primary culture. When 80%–90% confluence was reached, adherent cells were detached by trypsinization with 0.25% trypsin/ethylene diamine tetra acetic acid (EDTA) (Trypsin 1:250, EDTA 1 mM, Lonza Bioproducts, Belgium) and then were re-plated. The cultures were inspected daily for formation of adherent fusiform-shaped fibroblastoid cell. MSCs were labeled with a fluorescence marker using PKH26 Fluorescent Cell Linker Kit (Sigma- Aldrich), then injected into the rats.

### Detection of stem cells homing in lung tissues

Sections of lung tissue were examined using a fluorescent microscope (Olympus BX50F4, No.7M03285, Tokyo, Japan) to detect MSCs stained with PKH-26 in Medical Biochemistry and Molecular Biology Department, Faculty of Medicine, Zagazig University, Egypt.

### Biochemical assay

Multiple lung specimens were homogenized for detection of Nitric oxide (NO) and myeloperoxidase (MPO) activity that performed by spectrophotometry at 540 nm and 415 nm, respectively according to manufacturer's instruction as evidence of oxidative stress.

NO assay based on its rapid oxidation to nitrite and nitrate which are used to quantitate NO production (Kovács et al., 2015). MPO catalyzes the formation of reactive oxygen intermediates as hypochlorous acid from hydrogen peroxide (H<sub>2</sub>O<sub>2</sub>) and chloride anion (Aratani, 2018). The data were expressed as  $\mu\text{mole NO/g}$  and  $\text{nmol MPO/min/mL protein}$ .

Reduced glutathione (GSH) content in lung tissues was assayed according to manufacturer's instruction and to method described by (Ahmed et al., 1991) and measured spectrophotometrically at 412 nm. The data were expressed as  $\text{nmol GSH/mg protein}$ .

### Histopathological evaluation

#### Light microscopic study

Multiple lung sections were taken from each animal and fixed in 10% formalin and processed to prepare 5  $\mu\text{m}$  thick paraffin, some of sections were stained for Haematoxylin and Eosin (H & E) stain for histopathological evaluation (Bancroft and Gamble, 2008). Immunohistochemical staining was performed with anti-iNOS (Inducible nitric oxide synthase) (dilution 1: 50; Santa Cruz Biotechnology) using streptavidin–biotin immunoperoxidase technique (DakoCytomation, California, USA). Formalin-fixed, paraffin-embedded tissues were cut into (3- 4- $\mu\text{m}$ ) thick sections and transferred to 3-aminopropyltriethoxysilane (APTS) coated glass slides. The sections were subjected to dewaxing, rehydration, blocking with hydrogen peroxide, and antigen retrieval that was performed by heating specimens at 100°C for 20 min in citrate buffer (pH6.0) within microwave. One to two drops of the primary ready-to-use monoclonal antibody, anti-iNOS were then placed on the sections on separate slides. Slides were incubated at room temperature for 60 min. Incubation with secondary antibody and product visualization (Dako) was performed with DAB chromogen (3, 3'-diaminobenzidine tetrahydrochloride). Sections were counter-stained with hematoxylin, dehydrated with ethanol and xylene and mounted permanently with Din-butyl Phthalate in Xylene (DPX).

#### Transmission electron microscopic (TEM) study

Specimens were fixed in glutaraldehyde followed by fixation in osmium tetroxide. Then, they were dehydrated, embedded in resin. The ultrathin sections (Leica ultra-cut UCT) were stained with uranyl acetate and lead citrate (Ayache et al., 2010). Sections were

examined and photographed by (JEOL JEM1010 transmission electron microscope; Jeol Ltd., Tokyo, Japan) in the Regional Center of Mycology and Biotechnology (RCMB), Al- Azhar University, Egypt.

#### Statistical analysis

Results were expressed as mean  $\pm$  standard deviation (SD). Multi-group comparisons of the means were carried out by one-way analysis of variance (ANOVA) test. Least significant difference (LSD) test was used to compare the difference between the experimental groups and the control group. Probability values less than or equal to 0.05 were considered statistically significant (Craparo, 2007).

### 3. Results

#### Fluorescent microscope results

The lung tissues sections showed bright dots that represented the PKH-26 labeled cells.

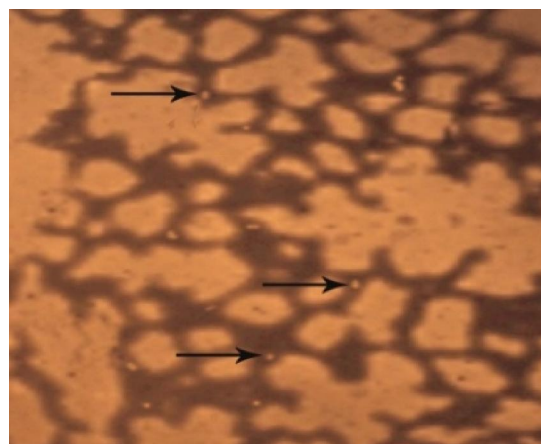


**Figure 1:** Lung tissue section of adult rats received HUCMSCs showed PKH-26 labeled cells (bright dots within the inter-alveolar septa (arrows)). (Fluorescent Microscope, X 200).

#### Biochemical assay results

The mean values of NO, MPO activities and GSH content in multiple sections of lung tissues showed non-significant differences between vehicle control groups B and C as compared to negative control group A ( $P > 0.05$ ).

Ag-NPs received rats showed highly significant increase in NO and MPO activity in lung tissues sections and reduction of GSH content of tissues as compared to control groups ( $P < 0.0001$ ).

After two daily successive intravenous doses of MSCs in Ag-NPs +MSCs showed highly significant reduction of NO, MPO activities and increment of GSH content of lung tissues sections as compared to Ag-NPs received group ( $P < 0.0001$ ), on the other hand, showed high significant differences as compared to control groups ( $P < 0.0001$ ) (Table 1).

**Table 1: Effects of HUCMSCs injection on biochemical analyses associated with Ag-NPs induced lung injury.**

Groups Parameter	Control groups Mean± SD			Ag-NPs group Mean± SD	Ag-NPs +MSCs Mean± SD	P value	F test
	A	B	C				
NO ( $\mu\text{mole/g}$ )	1.64±0.23	1.67±0.24	1.71±0.25	4.91± 0.53 <sup>a</sup>	2.47±0.23 <sup>bc</sup>	0.0001	89.789
MPO (nmol/min/mL)	2.07±0.29	2.04±0.35	2.17±0.31	6.48±0.68 <sup>a</sup>	2.98± 0.40 <sup>bc</sup>	0.0001	118.688
GSH (nmol/mg)	29.07±0.67	29.13±0.95	29.03±0.70	7.95±1.03 <sup>a</sup>	20.33±3.78 <sup>bc</sup>	0.0001	151.344

Values are expressed as means ±Standard Error (n=6), NO: Nitric oxide, MPO: Myeloperoxidase, GSH: Reduced glutathione,

a: highly significant difference as compared to control group ( $P < 0.0001$ ),

b: highly significant difference as compared to Ag-NPs received group ( $P < 0.0001$ ),

c: highly significant difference as compared to control group ( $P < 0.0001$ ).

## Histopathological results

### Light microscopic results

Examination of H & E stained lung tissues sections of control groups B and C showed the same normal histological architecture as compared to negative control (group A) that showed rounded or polygonal alveoli and alveolar sacs. The inter-capillaries were seen in the septa. Type I pneumocytes showed flat nuclei and type II pneumocytes showed rounded nuclei in the alveolar lining epithelium (**Figure 2 A, B**).

In Ag-NPs group, the lung sections showed areas with numerous collapsed alveoli and others with slightly patent alveoli. Marked peri-bronchial mononuclear inflammatory cell aggregates and fatty cellular infiltration were observed (**Figure 3A**), the inter-alveolar septa were thickened, the blood vessels were dilated, inflammatory cell aggregates were noticed and bundles of collagen fibers and exfoliated cells in the lumen were found (**Figure 3B**). The inter-alveolar septa showed numerous blood capillaries and acidophilic materials deposit or exudates were also noticed (**Figure 3C**). Numerous fat cells with peripheral compressed nuclei and abundant bundles of collagen fibers were demonstrated (**Figure 3D**).

With examination of the lung sections of Ag-NPs+HUCMSCs group, there were some features of recovery in the form of apparently normal alveoli and their sacs with some collapsed alveoli. Some of the inter-alveolar septa were thick and other septa were thin. Little congested and dilated blood vessels were also observed (**Figure 4A**). Numerous thin inter-alveolar septa with few thickened ones were seen. Types I and II pneumocytes with flat and rounded nuclei, respectively; were observed in the alveolar lining epithelium. However, hemorrhage was still found (**Figure 4B**).

While with examination of immunohistochemical staining of lung sections for iNOS of control groups B and C showed the same immunoreaction as compared to negative control (group A) where the alveolar walls and sacs showed weak positive expressions of iNOS (**Figure 5 A**). In Ag-NPs group, the lung sections showed strong positive expressions of iNOS in the alveolar walls and sacs (**Figure 5 B**). However, in Ag-NPs + HUCMSCs group, there were weak positive expressions of iNOS in the alveolar walls and sacs (**Figure 5 C**).

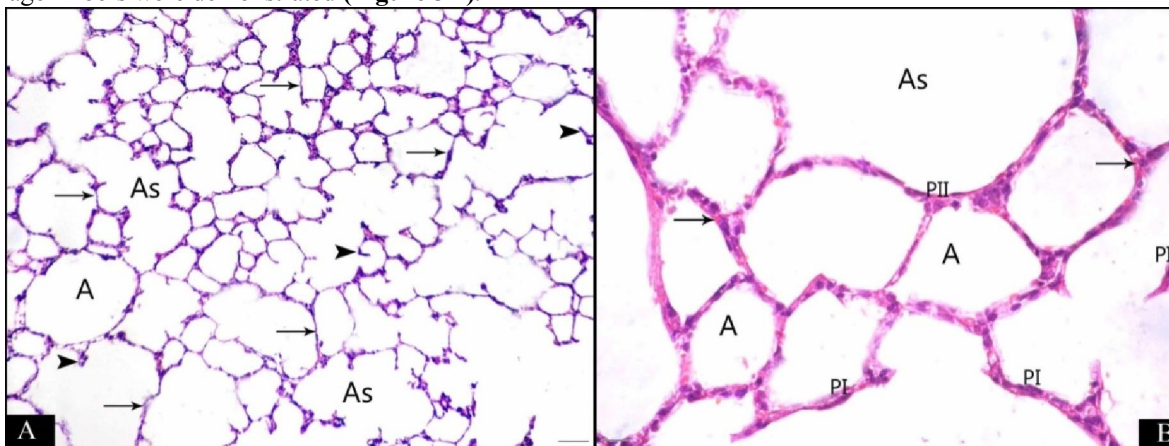


**Figure 2.** Photomicrographs of lung sections of Control groups. **A:** Normal lung architecture with rounded or polygonal alveoli (A), alveolar sacs (As). Both inter-alveolar (arrows) and prominent intra-alveolar septa (arrow head) are thin. **B:** Alveolar sac (As) and alveoli (A) with blood capillaries (arrows) in their septa are seen. Type I pneumocytes (PI) with flat nuclei and pneumocytes II (PII) with rounded nuclei are seen in the alveolar lining epithelium. (H & E x100 A, x400 B).

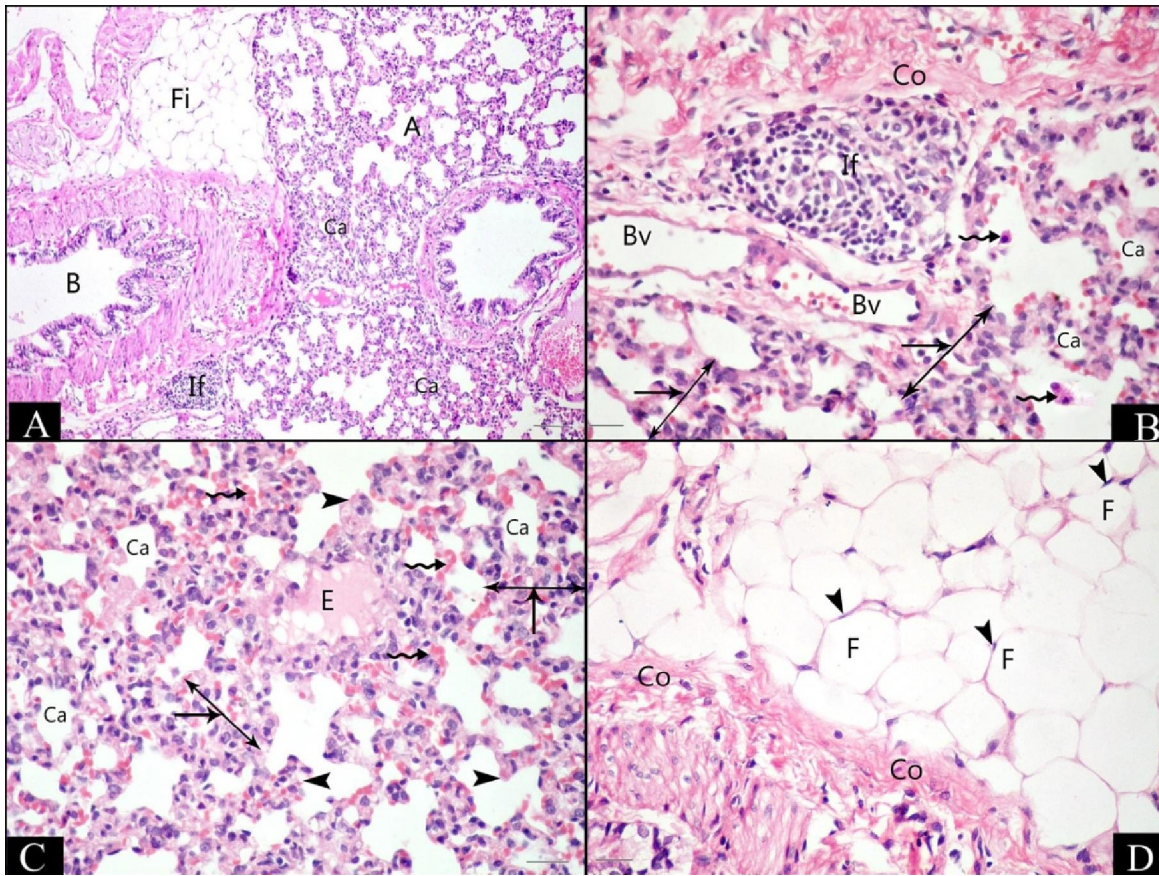


**Figure 3.** Photomicrographs of lung sections of Ag-NPs group. **A:** areas of obvious collapsed alveoli (Ca) and other with slightly patent alveoli (A). Marked peri-bronchial mononuclear inflammatory cell aggregates (If) around bronchiole (B) and fatty cellular infiltration (Fi) can be observed. **B:** Collapsed alveoli (Ca), thickened inter-alveolar septa (two head arrows), dilated blood vessels (Bv), inflammatory cell aggregates (If) and bundles of collagen fibers (Co) and exfoliated cells in lumen (wavy arrows) are observed. **C:** Numerous collapsed alveoli (Ca) and thickening of multiple inter-alveolar septa (two head arrows) are observed. Numerous blood capillaries (wavy arrows) are observed in these septa. Numerous thick intra-alveolar septa (arrow heads) and acidophilic materials or exudate (E) are also noticed. **D:** Numerous fat cells (F) with peripheral compressed nuclei (arrow heads) and abundant bundles of collagen fibers (Co) are demonstrated. (H & E x100 A; x400 B, C, D).

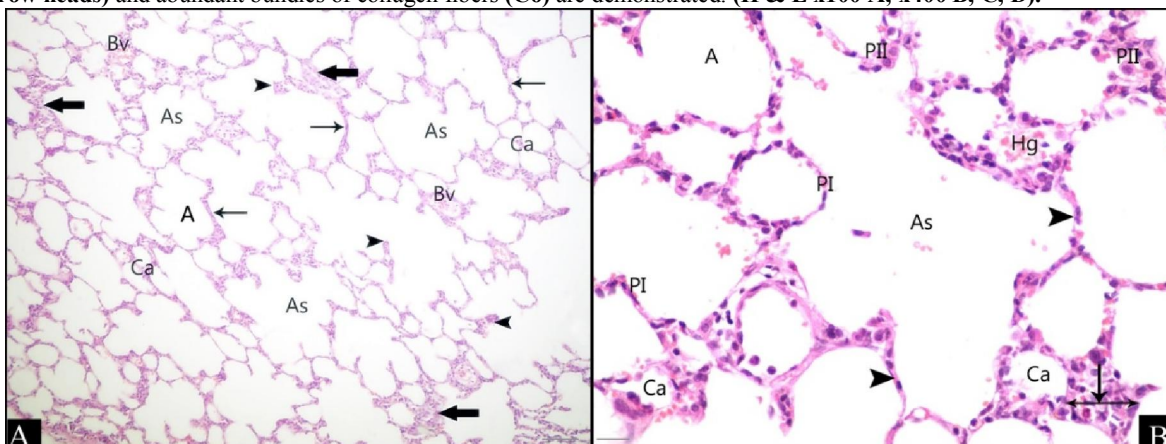


**Figure 4.** Photomicrographs of lung sections of Ag-NPs + HUCMSCs group. **A:** apparently normal alveoli (A) with their sacs (As) and some areas of collapsed alveoli (Ca) are seen. The inter-alveolar septa become thin (thin arrow), some septa show thickness (thick arrow) and thick intra-alveolar septa (arrowhead) are seen. Still dilated and congested blood vessels (Bv) are observed. **B:** normal apparent alveoli (A) and alveolar sac (As) with some collapsed alveoli (Ca) can be seen. Few thickened (arrow) and numerous thin inter-alveolar septa (arrow heads) are seen. Hemorrhage (Hg) is still observed. Types I pneumocytes (PI) with flat and II (PII) with rounded nuclei are seen in the alveolar lining epithelium. (H & E x100 A, x400 B).

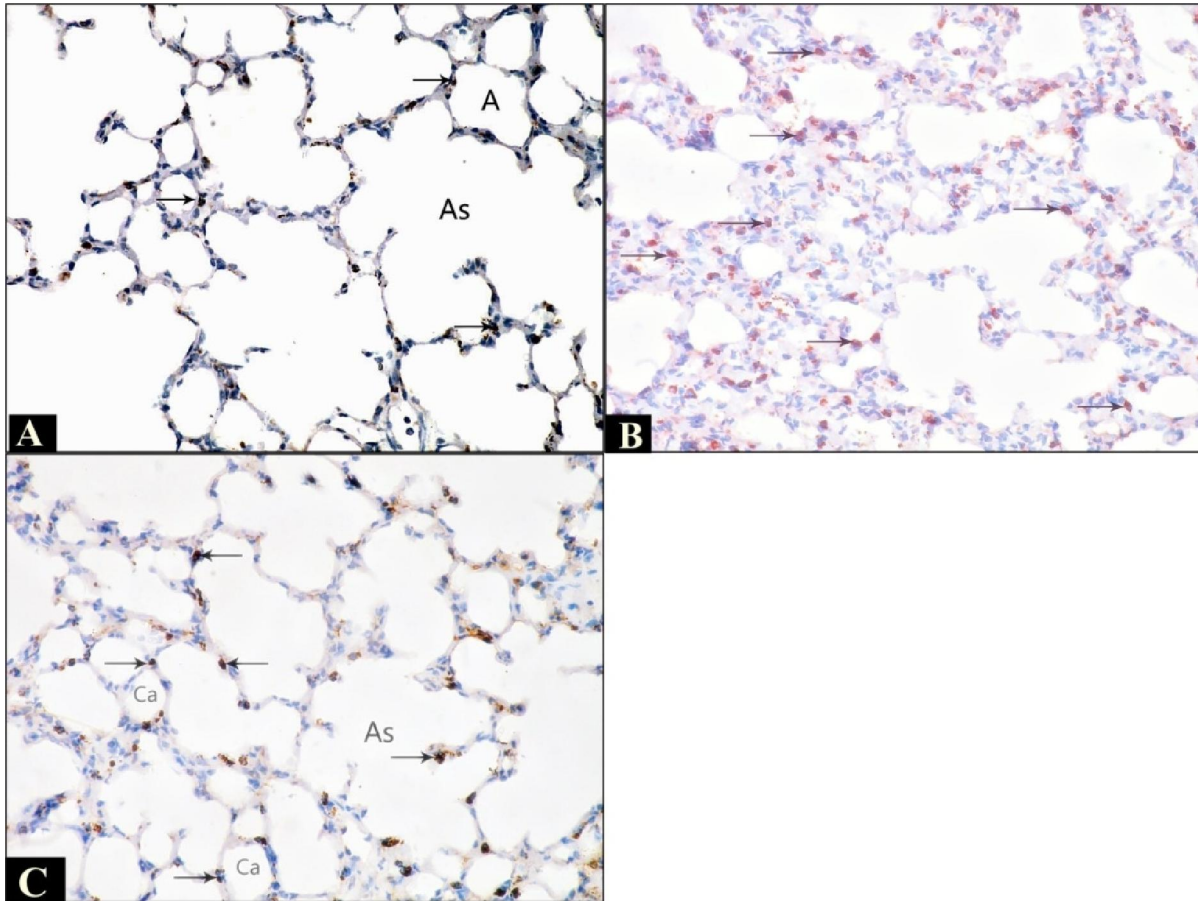


**Figure 5.** Photomicrographs of lung sections of different studied groups for iNOS immunoreactivity. **A:** lung sections of control group show weak positive expression of  $\alpha$ -SMA in alveolar wall (**A**) and sacs (**As**). **B:** lung sections of Ag-NPs group show strong positive expression in numerous cells (**arrows**) in thickened inter-alveolar septa. **C:** lung sections of Ag-NPs+ HUCMSCs group show weak positive reacted cells (**arrows**) in wall of some collapsed alveoli (**Ca**) and sacs (**As**). (**Immunohistochemical staining X400**).

#### Transmission electron microscopic (TEM) results

Electron microscopic (TEM) examination of control groups B and C showed the same normal ultra-structural architecture as compared to negative control (group A) that showed alveoli lined by thin inter-alveolar septa. The pneumocytes type I showed flat euchromatic nucleus (**Figure 6A**). While, Pneumocytes type II showed rounded euchromatic nucleus, defined lamellar bodies and numerous mitochondria. Well defined groups of interstitial cells with variable shaped nuclei were demonstrated (**Figure 6B**).

In Ag-NPs group, TEM examinations of lung sections showed altered ultra-structural architecture in the form of the inter-alveolar septa showed thickness, many interstitial cells with variable shaped and sized nuclei and collagen fibers. Pneumocyte type I was still

unaffected with flat nucleus while Pneumocyte type II showed either irregular heterochromatic nuclei or apoptotic small nuclei. The lamellar bodies were empty or destroyed forming vacuoles in the cytoplasm and in alveolar lumens. Some of thick inter-alveolar septa showed macrophages with small dense bodies and exudate and other septa showed abundant bundles of collagen fibers and flat interstitial cells or fibroblasts (**Figure 7 A, B, C, D**).

However in AgNPs +HUCMSCs group, TEM examinations of lung sections showed slight ultra-structural features of recovery, where the thickness of inter-alveolar septa was reduced, Pneumocytes type II showed normally apparent euchromatic nuclei and well defined lamellar bodies. Few collagen fibers and interstitial cells with irregular nuclei were still detected (**Figure 8 A, B**).

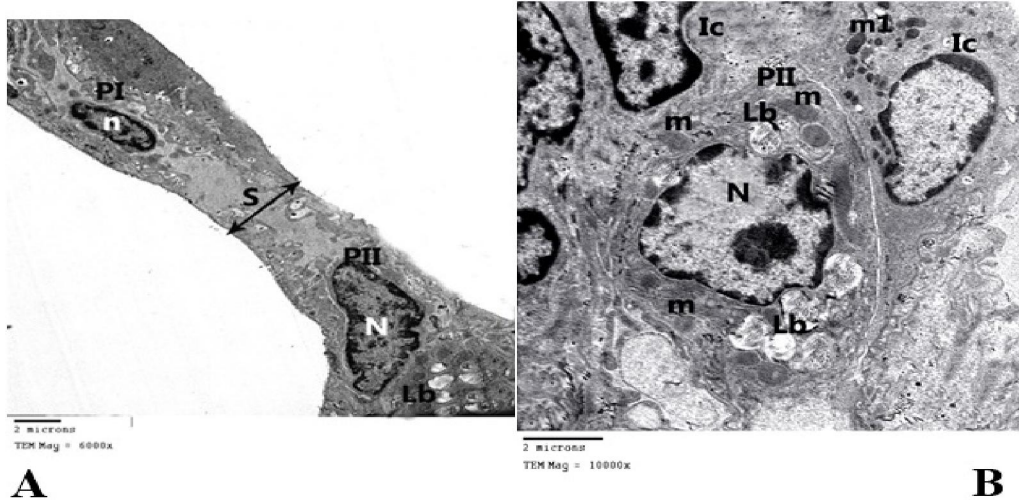


**Figure 6.** Photomicrographs of ultrathin lung sections of Control group. **A:** Alveoli lined by thin inter-alveolar septum (S) including pneumocytes types I (PI) with flat euochromatic nucleus (n) and type II (PII) with euochromatic nucleus (N) and lamellar bodies (Lb). **B:** Pneumocytes type II (PII) with rounded euochromatic nucleus (N), defined lamellar bodies (Lb) and many mitochondria (m) are demonstrated. Group of interstitial cells (Ic) with variable shaped nuclei and one contains numerous mitochondria (m1). (TEM. Mag. x 6000 (A) and x10000 (B))

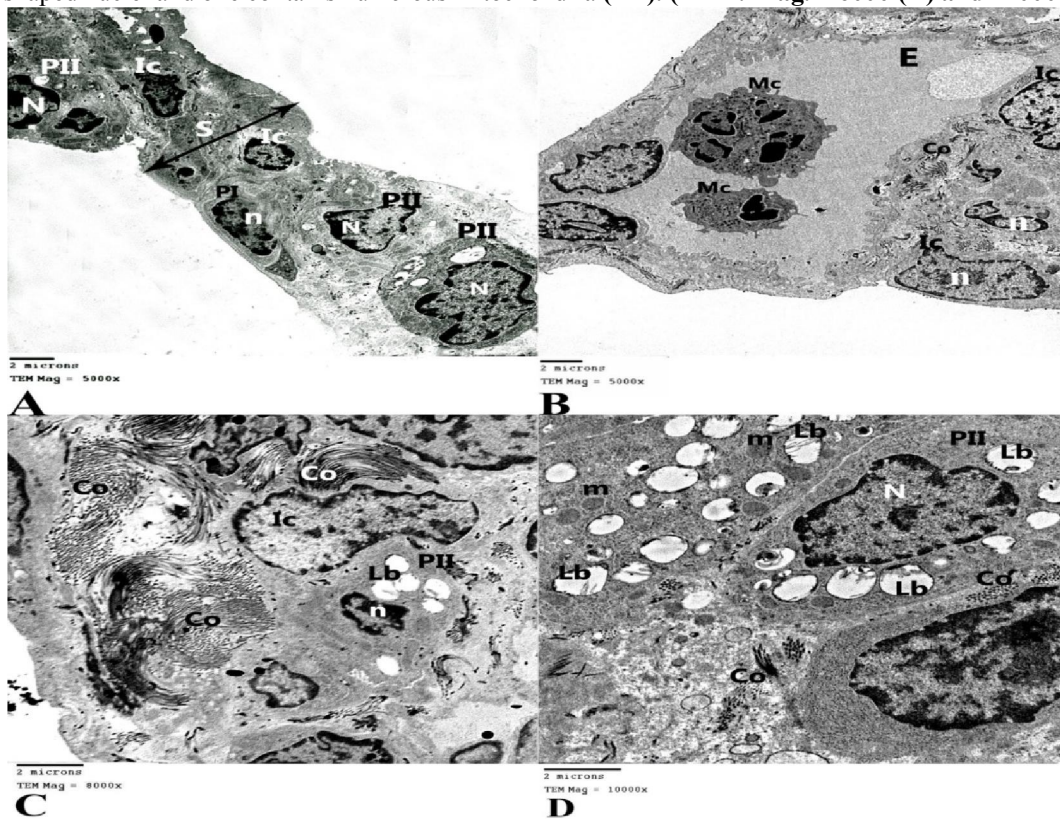


**Figure 7.** Photomicrographs of ultrathin lung sections of Ag-NPs group. **A:** the inter-alveolar septum (S) shows interstitial cells (Ic) with variable shaped nuclei, and Pneumocytes type II (PII) with irregular nucleus (N) while Pneumocyte type I (PI) still with flat nucleus (n). **B:** Thick inter-alveolar septa show macrophages (Mc) with small dense bodies and exudate (E). Group of interstitial cells (Ic) with variable shaped and sized nuclei (n) and collagen fibers (Co) could be found. **C:** Other thick inter-alveolar septum shows abundant bundles of collagen (Co). The Pneumocytes type II (PII) with apoptotic small nucleus (n) and empty lamellar bodies (Lb) forming vacuoles is seen. **D:** A thick septum reveals pneumocyte type II (PII) with irregular nucleus (N), mitochondria (m) and empty lamellar bodies (Lb) forming vacuoles in its cytoplasm could be demonstrated with collagen fibers (Co). (TEM. Mag. x 5000 (A, B), 8000 (C) and x10000 (D)).

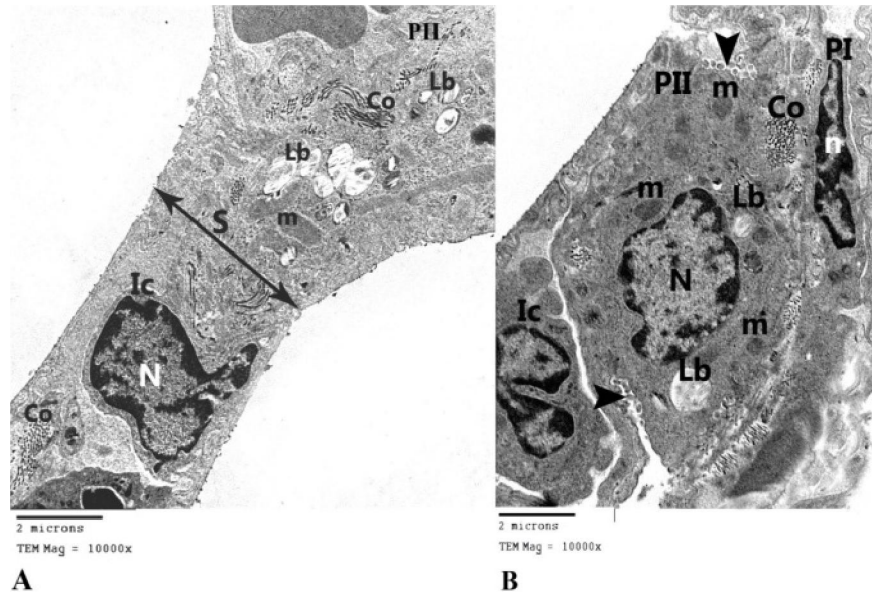


**Figure 8.** Photomicrographs of ultrathin lung sections of Ag-NPs +HUCMSCs group. **A:** Thin inter-alveolar septum (S) shows interstitial cell (Ic) with irregular shaped nucleus (N). Parts of Pneumocytes type II cytoplasm (PII) with defined lamellated bodies (Lb) and mitochondria (m). Few collagen fibers (Co) can be noticed. **B:** Pneumocytes type II (PII) with euchromatic nucleus (N), normally apparent lamellar bodies (Lb), mitochondria (m) and microvilli (arrow head) is well seen. Interstitial cell with irregular nucleus (Ic) and few collagen fibers (Co) can be observed and Pneumocytes type I (PI) still with flat nucleus (n). (TEM. Mag. x10000 A, B).

#### 4. Discussion

Addition of Ag-NPs to food packages and cosmetics was the motivation to study its effects on lung of adult rats especially; by oral route. The previous studies reported the cytotoxic effects of ingested Ag-NPs by releasing high concentrations of silver ions, that was referred to as the Trojan horse effect (Gliga et al., 2014) suggesting analysis of silver inside cells (Hsiao et al., 2015).

In the current study, the examination of lung tissues of adult rats for NO and MPO activities and GSH content after sub-chronic exposure to oral Ag-NPs showed highly significant increase in their activities and reduction of GSH content.

The in-vivo studies of ingested silver nanoparticles that affect the lung tissues of experimental animals were limited to compare our data. However, in general there were previous studies reported that Ag-NPs produced oxidative stress through several investigational analysis. A study was done by (Patlolla et al., 2015) who suggested that short-term oral administration of high doses of AgNPs (100 mg/kg) could increase reactive oxygen species (ROS) and lipid hydroperoxide. Another study with inhalational Ag-NPs exposure reported increased malondialdehyde (MDA) in bronchial lavage, suggesting oxidative injury and pulmonary inflammation that could lead to altered pulmonary mechanics (Seiffert et al., 2014). BraydichStolle et al. (2005) attributed the cytotoxic effect of nanomaterials

to disruption of mitochondrial function and induction of oxidative stress resulting in membrane damage and apoptosis.

In the present study, HUCMSCs injection for two successive days in Ag-NPs intoxicated rats showed significant reduction of NO and MPO activities and increased GSH content in lung tissues of adult rats.

These results were in agreement with (Li et al., 2012) who reported that HUCMSCs improving MPO activity in lung tissues of rats after induction of lung injury by lipopolysaccharide. It had been suggesting that the main source of ROS in lung tissues is neutrophils and macrophages based on that MPO is the main indicator of neutrophil infiltration (Haegens et al., 2009). Another study showed that bone marrow-MSCs injection was effective in improving the oxidative stress in Ecoli induced acute lung injury in mice by reducing MPO activity and increased GSH, superoxide dismutase (SOD), catalase (CAT) and glutathione peroxidase (GPx) in lung tissues suggesting the antioxidant role of MSCs (Shalaby et al., 2014).

Mesenchymal stem cells (MSCs) have some advantages that encourage researchers to evaluate its ameliorating role in several organ injuries and toxicities as it couldn't be easily recognized by expression of human leucocytic antigen in low amounts, no immune response could be detected in the recipient due to suppression of T cell proliferation (Lanzoni et al., 2008). It was conducted that MSCs

have therapeutic potential in lung diseases (Antunes et al., 2014), especially; Human umbilical cord-derived mesenchymal stem cells (HUCMSCs) which are considered suitable for clinical application due to easy collection, high cell vitality (Li et al., 2009), low immune response (Lee et al., 2014), and high ability for accelerating tissue repair (El Omar et al., 2014). Moreover, they have the potential efficacy in treatment of lung injury (Moodley et al., 2009).

In the current study, Ag-NPs administration for 4 weeks caused pathological alteration that appeared with H & E staining; areas of numerous collapsed alveoli, marked peri-bronchial mononuclear inflammatory cell aggregates, fatty cellular infiltration, the inter-alveolar septa were thickened, the blood vessels were dilated and congested, and bundles of collagen fibers and exfoliated cells in the lumen were found. On the other hand, with administration of HUCMSCs, there were some features of recovery as the alveoli appeared normal with their sacs and still some collapsed alveoli were found. The inflammatory aggregates weren't appeared any more. Types I and II pneumocytes with flat and rounded nuclei, respectively; were observed in the alveolar lining epithelium. Numerous inter-alveolar septa appeared thin. However, little congested and dilated blood vessels and few thickened inter-alveolar septa were still observed.

These results were in agreement with previous studies which reported that Ag-NPs in the lung caused high inflammatory potential and can lead to granulomatous lesions (Seiffert et al., 2016; Sung et al., 2009). Other study reported reduction in the tidal volume and minute volume, mixed inflammatory cell infiltrate and alveolar inflammation (Sung et al., 2008). Chuang et al., (2013) recorded that the morphological changes induced by Ag-NPs marked by lymphocyte and macrophage infiltrations and that what was happened in the current study. It was suggested that nanoparticles caused tissue injury by inducing inflammation and immune response (Wen et al., 2017).

There were limited studies on the effect of HUCMSCs on Ag-NPs induced lung injury. However, with intra-tracheal injection of HUCMSCs to study their role in acute lung injury induced by lipopolysaccharide, it was found that HUCMSCs improved survival and attenuated lung inflammation in mice (Zhu et al., 2017). Some previous studies suggested the therapeutic role of MSCs as it aggregated within the inflammatory site and differentiated to form endothelial and epithelium-like phenotype cells (Rojas et al., 2005), others attributed their role to their anti-apoptotic, anti-inflammatory, angiogenic and immunomodulatory properties (Kawai et al., 2015; Waszak et al., 2012). Moreover, it could

secrete cytoprotective agents that help in lung injury repair (Danchuk et al., 2011).

In the present study, the examination of immunohistochemical staining of lung sections for iNOS in Ag-NPs group, the lung sections showed strong positive expressions of iNOS in the alveolar walls and sacs. However, the HUCMSCs treatment produced weak positive expressions of iNOS.

Inducible nitric oxide synthase (iNOS) is from several enzymes that catalyzed formation of nitric oxide (NO) from L-arginine, both of iNOS and NO are important in many physiological and produced in several pathological conditions (Speranza et al., 2007). High production of NO levels that induced by increased iNOS out-put encourages the reaction with superoxide leading to formation of peroxynitrite and cell toxicity by oxidative stress (Mungrue et al., 2002). In the present work, the increased NO activity in lung tissues of Ag-NPs group was confirmed by over expression of iNOS in the same group emphasizing the oxidative stress occurrence.

The histopathological alteration of Ag-NPs were confirmed with TEM examination of lung ultrathin sections that revealed altered ultra-structural architecture in the form of thickened inter-alveolar septa, many interstitial cells with variable shaped and sized nuclei and collagen fibers. Pneumocyte type II showed either irregular heterochromatic nuclei or apoptotic small nuclei. The lamellar bodies were empty or destroyed forming vacuoles. Some of thick inter-alveolar septa showed macrophages with small dense bodies and exudate and other septa showed abundant bundles of collagen fibers and flat interstitial cell or fibroblast. However with HUCMSCs administration, there were some ultra-structural features of recovery as reduction of the thickness of inter-alveolar septa, Pneumocytes type II retained normally apparent euchromatic nuclei and well defined lamellar bodies.

The thickness of inter-alveolar septa was attributed to bundles of collagen that demonstrated in alveolar wall and that lead to modification of protein and carbohydrates composition (Rumble et al., 1997). Similarly, presence of macrophage in alveolar septa was attributed to scavenging of silver particles (Anderson et al., 2015).

The beneficial role of HUCMSCs in reducing collagen fibers in alveolar septa may be attributed to their paracrine mechanisms (Rojas et al., 2005) in which the HUCMSCs produced excessive amounts of interleukin 1 receptor antagonist that reduced inflammation and fibrosis induced lung injury (Ortiz et al., 2007). In additionally, MSCs reduced collagen and increased hyaluronic acid formation in fibroblasts (Kumai et al., 2010).

## Conclusion

From results of the present work, we concluded the harmful effects of sub-chronic oral exposure to Ag-NPs induced oxidative stress, histopathological and ultra-structural alteration in lung tissues of adult male rats and the tremendous role of HUCMSCs in improving the Ag-NPs detrimental effects by reducing MPO, NO activities that confirmed by decreasing iNOS expressing cells and increased GSH contents. Furthermore, they improved some of altered histopathological and ultra-structural changes.

## Conflict of Interests

The authors declared no potential conflicts of interest with respect to the research, authorship, and/or publication of this article.

## Funding

The author (s) received no financial support for the research, authorship, and/or publication of this article.

## References

- Ahmed, A.E., Hussein, G.I., Loh, J.P., Abdel-Rahman, S.Z., 1991. Studies on the mechanism of haloacetonitrile-induced gastrointestinal toxicity: interaction of dibromoacetonitrile with glutathione and glutathione-S-transferase in rats. *J. Biochem. Toxicol.* 6: 115-121. <https://doi.org/10.1002/jbt.2570060205>
- Anderson, D.S., Silva, R.M., Van Winkle, L.S., 2015. Persistence of Silver Nanoparticles in the Rat Lung: Influence of Dose, Size and Chemical Composition. *Nanotoxicology.* 9(5):591-602. <https://doi:10.3109/17435390.2014.958116>.
- Antunes, M.A., Laffey, J.G., Pelosi, P., Rocco, P.R.M., 2014. Mesenchymal Stem Cell Trials for Pulmonary Diseases. *Journal of Cellular Biochemistry.* 115(6): 1023-1032. <http://doi:10.1002/jcb.24783>.
- Aratani, Y., 2018. Myeloperoxidase: Its role for host defense, inflammation, and neutrophil function. *Archives of Biochemistry and Biophysics.* 640:47-52. <https://doi:10.1016/j.abb.2018.01.004>.
- Ayache, J., Beaunier, L., Boumendil, J., Ehret, G., Laub, D., 2010. Sample preparation handbook for transmission electron microscopy: techniques. New York USA: Springer Science & Business Media.
- Bancroft, J.D., Gamble, M., 2008. Connective tissue stains. In: Bancroft, J.D., Gamble, M., (Eds.), *Theory and Practice of Histological Techniques.* 6th ed. Elsevier Health Sciences, Churchill Livingstone; London, Oxford, New York, Philadelphia, St Louis, Sydney; pp. 150.
- Braydich Stolle, L., Hussain, S., Schlager, J.J., Hofmann, M.C., 2005. In vitro cytotoxicity of nanoparticles in mammalian germline stem cells. *Toxicological Sciences.* 88(2): 412-419. <https://doi:10.1093/toxsci/kfi256>.
- Chuang, H.C., Hsiao, T.C., Wu, C.K., Chang, H.H., Lee, C.H., Chang, C.C., Cheng, T., 2013. Allergenicity and toxicology of inhaled silver nanoparticles in allergen provocation mice models. *International journal of nanomedicine.* 8(1):4495-506. <https://doi.org/10.2147/IJN.S52239> PMID: 24285922; PubMed Central PMCID: PMC3841295.
- Craparo, R.M., 2007. Significance level. In Salkind, Neil, J. *Encyclopedia of Measurement and Statistics.* 3<sup>rd</sup> edition, Thousand Oaks, CA: SAGE Publications. pp. 889-891.
- Danchuk, S., Ylostalo, J.H., Hossain, F., Sorge, R., Ramsey, A., Bonvillain, R.W., 2011. Human multipotent stromal cells attenuate lipopolysaccharide-induced acute lung injury in mice via secretion of tumor necrosis factor-alpha-induced protein 6. *Stem. Cell Res. Ther.* 2(3):27. <https://doi:10.1186/scrt68>
- El Omar, R., Beroud, J., Stoltz, J.F., Menu, P., Velot, E., Decot, V., 2014. Umbilical Cord Mesenchymal Stem Cells: The New Gold Standard for Mesenchymal Stem Cell-Based Therapies? *Tissue Engineering Part B: Reviews.* 20(5): 523-544. <https://doi:10.1089/ten.TEB.2013.0664>.
- Gliga, A.R., Skoglund, S., Wallinder, I.O., Fadeel, B., Karlsson, H.L., 2014. Size-dependent cytotoxicity of silver nanoparticles in human lung cells: The role of cellular uptake, agglomeration and Ag release. *Part. Fibre Toxicol.* 11(1):11. <https://doi:10.1186/1743-8977-11-11>.
- Haegens, A., Heeringa, P., van Suylen, R.J., Aratani, Y., O'Donoghue, R.J., Mutsaers, S.E., Mossman, B.T., Wouters, E.F., Vernooy, J.H., 2009. Myeloperoxidase deficiency attenuates lipopolysaccharide-induced acute lung inflammation and subsequent cytokine and chemokine production. *J. Immunol.* 182:7990-7996. <http://doi:10.4049/jimmunol.0800377>. <http://www.jimmunol.org/content/jimmunol/182/12/7990.full.pdf>.
- Hsiao, I.L., Hsieh, Y.K., Wang, C. F., Chen, I.C., Huang, Y.J., 2015. Trojan-horse mechanism in the cellular uptake of silver nanoparticles verified by direct intra- and extracellular silver speciation

- analysis. *Environ. Sci. Technol.* 49:3813–3821. <https://doi.org/10.1021/es504705p>.
16. Iavicoli, I., Fontana, L., Leso, V., Bergamaschi, A., 2013. The effects of nanomaterials as endocrine disruptors. *International Journal of Molecular Sciences.* 14: 16732–16801. <https://doi.org/10.3390/ijms140816732>.
  17. Kawai, T., Katagiri, W., Osugi, M., Sugimura, Y., Hibi, H., Ueda, M., 2015. Secretomes from bone marrow-derived mesenchymal stromal cells enhance periodontal tissue regeneration. *Cytotherapy.* 17(4): 369–381. <https://doi.org/10.1016/j.jcyt.2014.11.009>.
  18. Kim, K.S., Sung, J.H., Ryu, H.R., Choi, B.G., Cho, H.S., Lee, J.K., Yu, I.J., 2012. Genotoxicity, acute oral and dermal toxicity, eye and dermal irritation and corrosion and skin sensitisation of silver nanoparticles. *Nanotoxicol.* 7 (5):953-960. <https://doi.org/10.3109/17435390.2012.676099>.
  19. Kolios, G., Moodley, Y., 2013. Introduction to stem cells and regenerative medicine. *Respiration.* 85: 3–10. <https://doi.org/10.1159/000345615>.
  20. Kovács, M., Kiss, A., Gönczi, M., Miskolczi, G., Seprényi, G., Kaszaki, J., Kohr, M.J., Murphy, E., Végh, Á., 2015. Effect of sodium nitrite on ischaemia and reperfusion-induced arrhythmias in anaesthetized dogs: is protein S-nitrosylation involved? *PLoS One.* 10(4):e0122243. <https://doi.org/10.1371/journal.pone.0122243>.
  21. Krause, D.S., Theise, N.D., Collector, M.I., Henegariu, O., Hwang, S., Gardner, R., Neutzel, S., Sharkis, S.J., 2001. Multi-organ, multi-lineage engraftment by a single bone marrow-derived stem cell. *Cell.* 105:369–377. [https://doi.org/10.1016/S0092-8674\(01\)00328-2](https://doi.org/10.1016/S0092-8674(01)00328-2)
  22. Kumai, Y., Kobler, J.B., Park, H., Galindo, M., Herrera, V.L.M., Zeitels, S.M.M., 2010. Modulation of vocal fold scar fibroblasts by adipose-derived stem/stromal cells. *Laryngoscope.* 120: 330-337. <https://doi.org/10.1002/lary.20753>.
  23. Lanzoni, G., Roda, G., Belluzzi, A., Roda, E., Bagnara, G.P., 2008. Inflammatory bowel disease: Moving toward a stem cell based therapy. *World J. Gastroenterol.* 14(29): 4616-4626. <http://doi.org/10.3748/wjg.14.4616>
  24. Lee, J.W., Gupta, N., Serikov, V., Matthay, M.A., 2009. Potential application of mesenchymal stem cells in acute lung injury. *Expert Opin Biol Ther.* 9(10):1259–1270. <https://doi.org/10.1517/14712590903213651>
  25. Lee, M., Jeong, S.Y., Ha, J., Kim, M., Jin, H.J., Kwon, S.J., Jeon, H.B., 2014. Low immunogenicity of allogeneic human umbilical cord blood-derived mesenchymal stem cells in vitro and in vivo. *Biochemical and Biophysical Research Communications.* 446(4): 983–989. <https://doi.org/10.1016/j.bbrc.2014.03.051>.
  26. Li, G., Zhang, X., Wang, H., Wang, X., Meng, C., Chan, C., Kung, H., 2009. Comparative proteomic analysis of mesenchymal stem cells derived from human bone marrow, umbilical cord, and placenta: Implication in the migration. *PROTEOMICS.* 9(1): 20–30. [http://dx.doi.org/10.1007/978-1-4614-0254-1\\_18](http://dx.doi.org/10.1007/978-1-4614-0254-1_18).
  27. Li, J., Li, D., Liu, X., Tang, S., Wei, F., 2012. Human umbilical cord mesenchymal stem cells reduce systemic inflammation and attenuate LPS-induced acute lung injury in rats. *Journal of Inflammation.* 9(1): 33. <http://doi.org/10.1186/1476-9255-9-33>.
  28. Moodley, Y., Atienza, D., Manuelpillai, U., Samuel, C.S., Tchongue, J., Ilancheran, S., Trounson, A., 2009. Human Umbilical Cord Mesenchymal Stem Cells Reduce Fibrosis of Bleomycin-Induced Lung Injury. *The American Journal of Pathology.* 175(1): 303–313. <https://doi.org/10.2353/ajpath.2009.080629>.
  29. Mungrue, I.N., Husain, M., Stewart, D.J., 2002. The role of NOS in heart failure: lessons from murine genetic model. *Heart Fail. Rev.* 7 (4): 407–422. [https://doi.org/10.1007/1-4020-7960-5\\_10](https://doi.org/10.1007/1-4020-7960-5_10).
  30. Ortiz, L.A., Dutreil, M., Fattman, C., Pandey, A.C., Torres, G., Go, K., Phinney, D.G., 2007. Interleukin 1 receptor antagonist mediates the antiinflammatory and antifibrotic effect of mesenchymal stem cells during lung injury. *Proc. Nat. Acad. Sci.* 104 (26): 11002–11007. <https://doi.org/10.1073/pnas.0704421104>.
  31. Patlolla, A.K., Hackett, D., Tchounwou, P.B., 2015. Silver nanoparticle-induced oxidative stress-dependent toxicity in Sprague-Dawley rats. *Molecular and cellular biochemistry.* 399(1–2):257–268. <https://doi.org/10.1007/s11010-014-2252-7>.
  32. Reidy, B., Haase, A., Luch, A., Dawson, K., Lynch, I., 2013. Mechanisms of Silver Nanoparticle Release, Transformation and Toxicity: A Critical Review of Current Knowledge and Recommendations for Future Studies and Applications. *Materials,* 6: 2295–2350. <https://doi.org/10.3390/ma6062295>.
  33. Rojas, M., Xu, J., Woods, C. R., Mora, A.L., Spears, W., Roman, J., Brigham, K.L., 2005. Bone Marrow-Derived Mesenchymal Stem Cells in Repair of the Injured Lung. *American Journal of Respiratory Cell and Molecular Biology,* 33(2):145–152. <https://doi.org/10.1165/rcmb.2004-0330oc>.

34. Rumble, J., Cooper, T., Leonard, W., Sherif, Y., Jermus, G., 1997. Vascular hypertrophy in experimental diabetes. Role of advanced glycation end products. *J. clin. Invest.* 99(5):1016-1027. <https://www.ncbi.nlm.nih.gov/pubmed/9062360>.
35. Secunda, R., Vennila, R., Mohanashankar, A.M., Rajasundari, M., Jeswanth, S., Surendran, R., 2015. Isolation, expansion and characterization of mesenchymal stem cells from human bone marrow, adipose tissue, umbilical cord blood and matrix: a comparative study. *Cyto Technology.* 67:793–807. <https://doi:10.1007/s10616-014-9718-z>
36. Seiffert, J., Hussain, F., Guo, C., Chang, Y., Zhang, J., Smith, R., Tetley, T., Chung, F., 2014. Inhaled silver nanoparticles induce pulmonary oxidative injury and inflammation: Differential effects between rat strains. *European Respiratory Journal.* 44 (58):3939. [http://erj.ersjournals.com/content/44/Suppl\\_58/P3939](http://erj.ersjournals.com/content/44/Suppl_58/P3939).
37. Seiffert, J., Hussain, F., Wiegman, C., Li, F., Bey, L., Baker, W., et al., 2015. Pulmonary Toxicity of Instilled Silver Nanoparticles: Influence of Size, Coating and Rat Strain. *PLoS ONE.* 10(3):e0119726. <https://doi.org/10.1371/journal.pone.0119726>.
38. Seiffert, J., Buckley, A., Leo, B., Martin, N.G., Zhu, J., Dai, R., Hussain, F., Guo, C., Warren, J., Hodgson, A., 2016. Pulmonary effects of inhalation of spark generated silver nanoparticles in Brown-Norway and Sprague-Dawley rats. *Respir. Res.* 17: 85. <https://doi:10.1186/s12931-016-0407-7>.
39. Shalaby, S.M., El-Shal, A.S., Abd-Allah, S.H., Selim, A.O., Selim, S.A., Gouda, Z.A., Abdelazim, S., 2014. Mesenchymal stromal cell injection protects against oxidative stress in *Escherichia coli*-induced acute lung injury in mice. *Cytotherapy.* 16(6): 764–775. <https://doi.org/10.1016/j.jcyt.2013.12.006>.
40. Speranza, L., De Lutiis, M.A., Shaik, Y.B., Felaco, M., Patruno, A., Tetè, S., Tetè, A., Mastrangelo, F., Madhappan, B., Castellani, M.L., Conti, F., Vecchiet, J., Theoharides, T.C., Conti, P., Grilli, A., 2007. Localization and activity of iNOS in normal human lung tissue and lung cancer tissue. *Int. J. Biol. Markers.* 22(3):226-231. <https://doi:10.1177/172460080702200311>.
41. Sung, J.H., Ji, J.H., Yun, J.U., Kim, D.S., Song, M.Y., Jeong, J., Han, B.S., Han, J.H., Chung, Y.H., Kim, J., 2008. Lung function changes in Sprague-Dawley rats after prolonged inhalation exposure to silver nanoparticles. *Inhal. Toxicol.* 20(6): 567–574. <https://doi.org/10.1080/08958370701874671>.
42. Sung, J.H., Ji, J.H., Park, J.D., Yoon, J.U., Kim, D.S., Jeon, K.S., Song, M.Y., Jeong, J., Han, B.S., Han, J.H., 2009. Subchronic inhalation toxicity of silver nanoparticles. *Toxicol. Sci.* 108(2) 452–461. <https://doi:10.1093/toxsci/kfn246>.
43. Waszak, P., Alphonse, R., Vadivel, A., Ionescu, L., Eaton, F., Thébaud, B., 2012. Preconditioning Enhances the Paracrine Effect of Mesenchymal Stem Cells in Preventing Oxygen-Induced Neonatal Lung Injury in Rats. *Stem Cells and Development.* 21(15): 2789–2797. <https://doi:10.1089/scd.2010.0566>.
44. Wen, H., Dan, M., Yang, Y., Lyu, J., Shao, A., Cheng, X., Chen, L., Xu, L., 2017. Acute toxicity and genotoxicity of silver nanoparticle in rats. *PLoS ONE.* 12(9): e0185554. <https://doi.org/10.1371/journal.pone.0185554>.
45. Wiemann, M., Vennemann, A., Blaske, F., Sperling, M., Karst, U., 2017. Silver Nanoparticles in the Lung: Toxic Effects and Focal Accumulation of Silver in Remote Organs. *Nanomaterials.* 7:441. <https://doi:10.3390/nano7120441>.
46. Wijnhoven, S.W.P., Peijnenburg, W.J.G.M., Herberts, C.A., Hagens, W.I., Oomen, A.G., Heugens, E.H.W., Roszek, B., Bisschops, J., Gosens, I., Van De Meent, D., et al., 2009. Nano-silver—A review of available data and knowledge gaps in human and environmental risk assessment. *Nanotoxicology.* 3: 109–138. <https://doi.org/10.1080/17435390902725914>.
47. Xia, T., Kovochich, M., Lion, M., Madler, L., Gilbert, B., Shi, H., Yeh, J.I., Zink, J.I., Nel, A.E., 2008. Comparison of the mechanism of toxicity of zinc oxide and cerium oxide nanoparticles based on dissolution and oxidative stress properties. *ACS Nano.* 2 (10):2121–2134. <https://doi:10.1021/nm800511k>.
48. Zhu, H., Xiong, Y., Xia, Y., Zhang, R., Tian, D., Wang, T., 2017. Therapeutic effects of human umbilical cord-derived mesenchymal stem cells in acute lung injury mice. *Scientific Reports.* 7(1): 39889. <https://doi:10.1038/srep39889> accessed on 15 Jan 2018.